

## Critical mass of Wilson fermions: A comparison of perturbative and Monte Carlo results

E. Follana\* and H. Panagopoulos†

*Department of Physics, University of Cyprus, P.O. Box 20537, Nicosia CY-1678, Cyprus*

(Received 1 June 2000; published 4 December 2000)

We calculate the critical value of the hopping parameter,  $\kappa_c$ , in lattice QCD with Wilson fermions, to two loops in perturbation theory. This quantity is an additive renormalization; as such, it is characterized not only by the standard caveats regarding the asymptotic nature of perturbative results, but also by a linear divergence in the lattice spacing. Consequently, our calculation tests rather stringently the limits of applicability of perturbation theory. We compare our results to non-perturbative evaluations of  $\kappa_c$  coming from Monte Carlo simulations. Finally, we apply a tadpole improvement technique to our results; this shifts them quite favorably towards the nonperturbative values.

DOI: 10.1103/PhysRevD.63.017501

PACS number(s): 12.38.Gc, 11.10.Gh, 11.15.Ha

In this paper we study the hopping parameter in lattice QCD with Wilson fermions. In particular, we compute its critical value to two loops in perturbation theory.

Wilson fermions are the most straightforward and widely used implementation of fermionic actions on the lattice. This implementation circumvents the fermion doubling problem by introducing a higher derivative term with a vanishing classical continuum limit, to lift unphysical propagator poles completely. At the same time, the action is strictly local, which is very advantageous for numerical simulation.

The price one pays for strict locality and absence of doublers is well known: The higher derivative term breaks chiral invariance explicitly. Thus, merely setting the bare fermionic mass to zero is not sufficient to ensure chiral symmetry in the quantum continuum limit; quantum corrections introduce an additive renormalization to the fermionic mass, which must then be fine-tuned to have a vanishing renormalized value. Consequently, the hopping parameter  $\kappa$ , which is simply related to the fermion mass, must be appropriately shifted from its naive value, to recover chiral invariance.

By dimensional power counting, the additive mass renormalization is seen to be linearly divergent with the lattice spacing. This adverse feature of Wilson fermions poses an additional problem to a perturbative treatment, aside from the usual issues related to a lack of Borel summability. Indeed, our calculation serves as a check on the limits of applicability of perturbation theory, by comparison with non-perturbative results coming from Monte Carlo simulations.

Starting from our two-loop results, we also provide improved estimates of the critical value of  $\kappa$ , by performing a resummation to all orders of cactus diagrams [1]. These are tadpole-like diagrams which are gauge invariant and dress the propagators and vertices in our calculation. This improvement technique, among others, has so far been applied mostly to the one-loop multiplicative renormalization of various operators [2,3]. It is interesting to explore to what extent such methods lead to an improvement even in a sensitive case such as the one at hand. We find that our improved estimates compare quite well with Monte Carlo data also in this case.

QCD with Wilson fermions on the lattice is described by the following action (see, e.g., Ref. [4] notation):

$$S_L = \frac{1}{g_0^2} \sum_{x,\mu,\nu} \text{Tr}[1 - U_{\mu\nu}(x)] + \sum_{i=1}^{N_f} \sum_{x,y} \bar{\psi}_i(x) D(x,y) \psi_i(y). \quad (1)$$

$U_{\mu\nu}(x)$  is the standard product of link variables  $U_{x,y}$  around a plaquette in the direction  $\mu - \nu$ , originating at point  $x$ , and  $D(x,y)$  is given by

$$D(x,y) = am_B \delta_{x,y} + \frac{1}{2} \sum_{\mu} [\gamma_{\mu}(U_{x,y} \delta_{x+\hat{\mu},y} - U_{x,y} \delta_{x,y+\hat{\mu}}) - r(U_{x,y} \delta_{x+\hat{\mu},y} - 2\delta_{x,y} + U_{x,y} \delta_{x,y+\hat{\mu}})]. \quad (2)$$

As usual,  $g_0$  denotes the bare coupling constant and  $a$  is the lattice spacing. The bare fermionic mass  $m_B$  must be set to zero for chiral invariance in the classical continuum limit.

The higher derivative term, multiplied by the Wilson coefficient  $r$ , breaks chiral invariance. It vanishes in the classical continuum limit; at the quantum level, it induces nonzero, flavor-independent corrections to the fermion masses.

Numerical simulation algorithms usually employ the hopping parameter,  $\kappa \equiv 1/(2m_B a + 8r)$ , as a tunable quantity. Its critical value, at which chiral symmetry is restored, is thus  $1/8r$  classically, but gets shifted by quantum effects.

The renormalized mass can be calculated in textbook fashion from the fermion self-energy. Denoting by  $\Sigma^L(p, m_B, g_0)$  the one particle irreducible fermionic two-point function, we have, for the fermionic propagator,

$$S(p) = [i\hat{p} + m(p) - \Sigma^L(p, m_B, g_0)]^{-1} \quad (3)$$

where

$$\hat{p} = \sum_{\mu} \gamma_{\mu} \frac{1}{a} \sin(ap^{\mu}), \quad m(p) = m_B + \frac{2r}{a} \sum_{\mu} \sin^2(ap^{\mu}/2).$$

Requiring that the renormalized mass vanish leads one to  $S^{-1}(0) = 0 \Rightarrow m_B = \Sigma^L(0, m_B, g_0)$ . The above is a recursive equation for  $m_B$ , which can be solved order by order in perturbation theory.

\*Email address: eduardo@dirac.ns.ucy.ac.cy

†Email address: haris@ucy.ac.cy

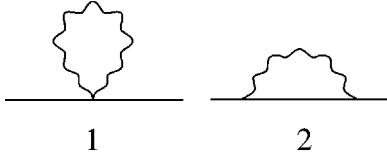


FIG. 1. One-loop diagrams contributing to  $\Sigma^L$ . Wavy (solid) lines represent gluons (fermions).

We write the loop expansion of  $\Sigma^L$  as  $\Sigma^L(0, m_B, g_0) = g_0^2 \Sigma^{(1)} + g_0^4 \Sigma^{(2)} + \dots$ . Figure 1 shows the two diagrams contributing to the 1-loop result  $\Sigma^{(1)}$ . The fermion mass involved in these diagrams must be set to its tree level value,  $m_B \rightarrow 0$ . The  $i^{\text{th}}$  diagram gives a contribution of the form  $[(N^2 - 1)/N] c_i^{(1)}$ , where  $c_1^{(1)}, c_2^{(1)}$  are numerical constants.

A total of 26 diagrams contribute to the 2-loop quantity  $\Sigma^{(2)}$ , shown in Fig. 2. Genuine 2-loop diagrams must again be evaluated at  $m_B \rightarrow 0$ ; in addition, one must include to this order the 1-loop diagram containing an  $\mathcal{O}(g_0^2)$  mass counterterm (diagram 23). The contribution of each diagram can be written in the form

$$(N^2 - 1)[c_{1,i}^{(2)} + (c_{2,i}^{(2)}/N^2) + (N_f/N) c_{3,i}^{(2)}] \quad (4)$$

where  $c_{1,i}^{(2)}, c_{2,i}^{(2)}, c_{3,i}^{(2)}$  are numerical constants. Certain sets of diagrams, corresponding to renormalization of loop propaga-

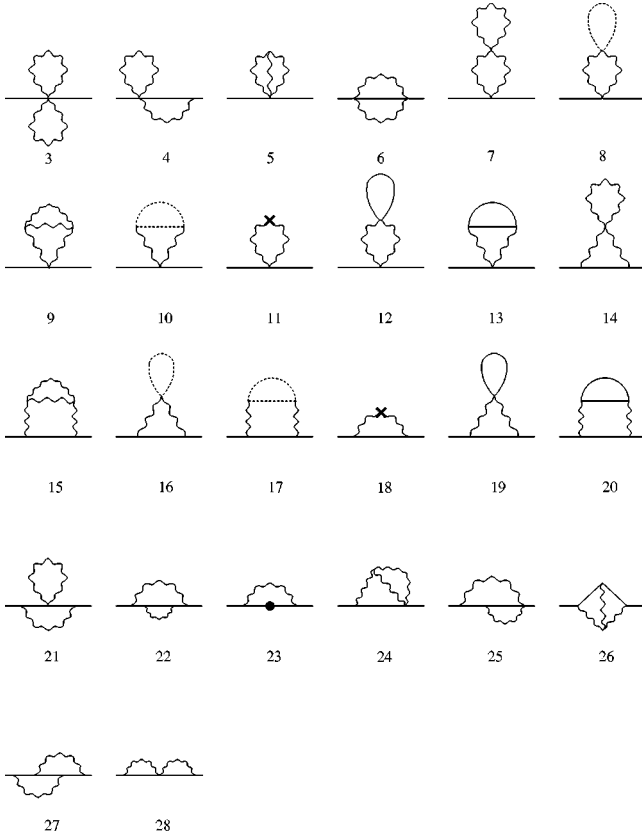


FIG. 2. Two-loop diagrams contributing to  $\Sigma^L$ . Wavy (solid, dotted) lines represent gluons (fermions, ghosts). Crosses denote vertices stemming from the measure part of the action; the solid circle is a fermion mass counterterm.

TABLE I. Coefficients  $c_i^{(1)}$ .  $r=1$ .

$i$	$c_i^{(1)}$
1	-0.15493339023106
2	-0.007923668480(2)

tors, must be evaluated together in order to obtain an infrared-convergent result: these are diagrams 7+8+9+10+11, 12+13, 14+15+16+17+18, 19+20, 21+22+23.

The evaluation of the diagrams in this computation requires very extensive analytical work. To this end, we use a MATHEMATICA package which we have developed for symbolic manipulations in lattice perturbation theory (see, e.g., Ref. [5]). Applied to the present case, this package allows us to perform the following tasks: Contraction among the appropriate vertices; simplification of color and Dirac matrices; use of trigonometry and momentum symmetries for reduction to a more compact, canonical form; automatic generation of highly optimized FORTRAN code for the loop integration of each type of expression.

The integrals, typically consisting of a sum over a few hundred trigonometric products, are then performed numerically on lattices of varying finite size  $L$ . Our programs perform extrapolations of each expression to a broad spectrum of functional forms of the type  $\sum_{i,j} e_{ij} (\ln L)^j / L^i$ , analyze the quality of each extrapolation using a variety of criteria and assign statistical weights to them, and finally produce a quite reliable estimate of the systematic error. Taking  $L \leq 28$  leads to a sufficient number of significant digits in our results.

One important consistency check can be performed on those diagrams which are separately IR divergent; taken together in groups, as listed below Eq. (4), they give a finite and very stable extrapolation.

We present below the numerical values of the constants  $c_i^{(1)}, c_{1,i}^{(2)}, c_{2,i}^{(2)}, c_{3,i}^{(2)}$ . These constants depend only on the Wilson parameter  $r$ ; following common practice, we set  $r=1$ .

Table I contains the contributions to the 1-loop quantity  $\Sigma^{(1)}$ . The total 1-loop result is

$$\Sigma^{(1)} = [(N^2 - 1)/N] [-0.162857058711(2)]. \quad (5)$$

This result is known in the literature (see, e.g., Ref. [6], p. 246, and references contained therein).

The contributions to the 2-loop quantity  $\Sigma^{(2)}$  are presented in Table II. The total 2-loop result is

$$\begin{aligned} \Sigma^{(2)} = & (N^2 - 1)[-0.017537(3) + (1/N^2)0.016567(2) \\ & + (N_f/N)0.00118618(8)]. \end{aligned} \quad (6)$$

In order to make a comparison with numerical simulations, let us set  $N=3, N_f=2$  in the above; we obtain

$$\Sigma^{(1)}(N=3, N_f=2) = -0.434285489897(5) \quad (7)$$

$$\Sigma^{(2)}(N=3, N_f=2) = -0.11925(3). \quad (8)$$

In Table III we list the final results for  $m_c^{(1)} = g_0^2 \Sigma^{(1)}$  and  $m_c^{(2)} = g_0^2 \Sigma^{(1)} + g_0^4 \Sigma^{(2)}$  in the quenched case ( $N_f=0$ ), along

TABLE II. Coefficients  $c_{1,i}^{(2)}$ ,  $c_{2,i}^{(2)}$ ,  $c_{3,i}^{(2)}$ .  $r=1$ .

$i$	$c_{1,i}^{(2)}$	$c_{2,i}^{(2)}$	$c_{3,i}^{(2)}$
3	0.002000362950707492	-0.0030005444260612375	0
4	0.00040921361(1)	-0.00061382041(2)	0
5	0	0	0
6	-0.0000488891(8)	0.000097778(2)	0
7+8+9+10+11	-0.013927(3)	0.014525(2)	0
12+13	0	0	0.00079263(8)
14+15+16+17+18	-0.005753(1)	0.0058323(7)	0
19+20	0	0	0.000393556(7)
21+22+23	0.000096768(4)	-0.000096768(4)	0
24	0	0	0
25	0.00007762(1)	-0.00015524(3)	0
26	-0.00040000(5)	0	0
27	0	-0.000006522(1)	0
28	0.0000078482(5)	-0.000015696(1)	0

with numerical simulation data at values of  $\beta=6/g_0^2$  equal to 5.7 [7], 6.0 [8], 6.1, 6.3 [9]; in Table IV we compare our results at  $N_f=2$  with numerical simulation data at  $\beta=5.6$  [10] and  $\beta=5.5$  [11]. Also included in these tables are the improved results obtained with the method described in the following section. For easier reference, Table V presents our results in terms of the critical hopping parameter  $\kappa_c = 1/(2m_c a + 8r)$ .

In order to obtain improved estimates from lattice perturbation theory, one may perform a resummation to all orders of the so-called ‘‘cactus’’ diagrams [1–3]. Briefly stated, these are gauge-invariant tadpole diagrams which become disconnected if any one of their vertices is removed. The original motivation of this procedure is the well known observation of ‘‘tadpole dominance’’ in lattice perturbation theory. In the following we refer to Ref. [1] for definitions and analytical results.

Since the contribution of standard tadpole diagrams is not gauge invariant, the class of gauge invariant diagrams we are considering needs further specification. By the Baker-Campbell-Hausdorff (BCH) formula, the product of link variables along the perimeter of a plaquette can be written as

$$\begin{aligned}
 U_{x,\mu\nu} &= e^{ig_0 A_{x,\mu}} e^{ig_0 A_{x+\mu,\nu}} e^{-ig_0 A_{x+\nu,\mu}} e^{-ig_0 A_{x,\nu}} \\
 &= \exp\{ig_0 F_{x,\mu\nu}^{(1)} + ig_0^2 F_{x,\mu\nu}^{(2)} + \mathcal{O}(g_0^4)\}. \quad (9)
 \end{aligned}$$

TABLE III.  $m_c^{(1)}$  and  $m_c^{(2)}$ .  $N=3$ ,  $N_f=0$ ,  $r=1$ .

	$\beta=5.7$	$\beta=6.0$	$\beta=6.1$	$\beta=6.3$
$m_c^{(1)}$	-0.457142620944(5)	-0.434285489897(5)	-0.427166055636(5)	-0.413605228473(5)
$m_c^{(2)}$	-0.59628(3)	-0.55986(3)	-0.54865(3)	-0.52750(2)
$m_{c,\text{dressed}}^{(1)}$	-0.624018239510(7)	-0.579221156426(6)	-0.565793230023(6)	-0.540845487886(6)
$m_{c,\text{dressed}}^{(2)}$	-0.73126(6)	-0.67162(5)	-0.65395(5)	-0.62140(4)
$\alpha_{\overline{\text{MS}}}(q^*)$	-0.93	-0.78	-0.75	-0.70
$\alpha_V(q^*)$	-1.12	-0.91	-0.86	-0.79
Simulation	-1.04(2)	-0.8181(2)	-0.7746(4)	-0.7066(4)

The diagrams that we propose to resum to all orders are the cactus diagrams made of vertices containing  $F_{x,\mu\nu}^{(1)}$ . These diagrams dress the transverse gluon propagator  $P_A$  leading to an improved propagator  $P_A^{(I)}$ , which is a multiple of the bare transverse one:

$$P_A^{(I)} = P_A / [1 - w(g_0)], \quad (10)$$

where the factor  $w(g_0)$  will depend on  $g_0$  and  $N$ , but not on the momentum. The function  $w(g_0)$  can be extracted by an appropriate algebraic equation that has been derived in Ref. [1] and that can be easily solved numerically; for  $SU(3)$ ,  $w(g_0)$  satisfies

$$ue^{-u/3}[u^2/3 - 4u + 8] = 2g_0^2, \quad u(g_0) \equiv \frac{g_0^2}{4[1 - w(g_0)]}. \quad (11)$$

The vertices coming from the gluon part of the action, Eq. (1), get also dressed using a procedure similar to the one leading to Eq. (10) [1]. Vertices coming from the fermionic action stay unchanged, since their definition contains no plaquettes on which to apply the linear BCH formula.

One can apply the resummation of cactus diagrams to the calculation of additive and multiplicative renormalizations of lattice operators. Applied to a number of cases of interest [1,2], this procedure yields remarkable improvements when

TABLE IV.  $m_c^{(1)}$  and  $m_c^{(2)}$ .  $N=3$ ,  $N_f=2$ ,  $r=1$ .

	$\beta=5.5$	$\beta=5.6$
$m_c^{(1)}$	-0.473765988978(5)	-0.465305882032(5)
$m_c^{(2)}$	-0.61568(3)	-0.60219(3)
$m_{c,\text{dressed}}^{(1)}$	-0.658392965489(7)	-0.640695803682(7)
$m_{c,\text{dressed}}^{(2)}$	-0.76323(6)	-0.73997(6)
Simulation	-0.897(3)	-0.8456(9)

compared with the available nonperturbative estimates. As regards numerical comparison with other improvement schemes (tadpole improvement, boosted perturbation theory, etc.) [12,13], cactus resummation fares equally well on all the cases studied [3].

One advantageous feature of cactus resummation, in comparison to other schemes of improved perturbation theory, is the possibility of systematically incorporating higher loop diagrams. The present calculation best exemplifies this feature, as we will now show.

Dressing the 1-loop result is quite straightforward: the fermionic propagator and vertices stay unchanged, and only the gluon propagator gets simply multiplied by  $1/(1-w(g_0))$ . The resulting values,  $m_{c,\text{dressed}}^{(1)}$  and  $\kappa_{c,\text{dressed}}^{(1)}$ , are shown in Tables IV and V, respectively. It is worth noting that these values already fare better than the much more cumbersome undressed 2-loop results.

We now turn to dressing the 2-loop results. Here, one must take care to avoid double counting: A part of diagrams 7 and 14 has already been included in dressing the 1-loop result, and must be explicitly subtracted from  $\Sigma^{(2)}$  before dressing. Fortunately, this part (we shall denote it by  $\Sigma_{\text{sub}}^{(2)}$ ) is easy to identify, as it necessarily includes all of the  $1/N^2$  part in  $\Sigma^{(2)}$ . A simple exercise in contraction of  $SU(N)$  generators shows that  $\Sigma_{\text{sub}}^{(2)}$  is proportional to  $(2N^2-3)(N^2-1)/(3N^2)$ . There follows immediately that  $\Sigma_{\text{sub}}^{(2)} = -0.016567(2N^2-3)(N^2-1)/(3N^2)$  [cf. Eq. (6)].

A further complication is presented by gluon vertices. While the 3-gluon vertex dresses by a mere factor of  $[1-w(g_0)]$ , the dressed 4-gluon vertex contains a term which

TABLE V.  $\kappa_c^{(1)}$  and  $\kappa_c^{(2)}$ .  $N=3$ ,  $N_f=2$ ,  $r=1$ .

	$\beta=5.5$	$\beta=5.6$
$\kappa_c^{(1)}$	0.1417943331149(4)	0.1414549557367(4)
$\kappa_c^{(2)}$	0.147740(3)	0.147154(3)
$\kappa_{c,\text{dressed}}^{(1)}$	0.1496286052897(6)	0.1488403463277(6)
$\kappa_{c,\text{dressed}}^{(2)}$	0.154475(6)	0.153373(6)
Simulation	0.16116(15)	0.158507 <sup>+41</sup> <sub>-44</sub>

is not simply a multiple of its bare counterpart (see Appendix C of Ref. [1]). Once again, however, we are fortunate: this term must be dropped, being precisely the one which has already been taken into account in dressing the 1-loop result, while the remainder dresses in the same way as the 3-gluon vertex. In conclusion, cactus resummation applied to the 2-loop quantity  $\Sigma^{(2)}$  leads to the following recipe:

$$m_{c,\text{dressed}}^{(2)} = \Sigma^{(1)} \frac{g_0^2}{1-w(g_0)} + (\Sigma^{(2)} - \Sigma_{\text{sub}}^{(2)}) \frac{g_0^4}{[1-w(g_0)]^2}.$$

[For the particular values of  $\beta$  used in the tables,  $\beta = 5.5, 5.6, 5.7, 6.0, 6.1, 6.3$ , we obtain, from Eq. (11),  $1-w(g_0) = 0.719579, 0.726251, 0.732579, 0.749775, 0.754986, 0.764738$ , respectively.]

In Table III we present, at various values of  $\beta$  and  $N_f = 0$ , our results for  $m_c$  (at one and two loops, with and without cactus dressing), results taken from Ref. [13] [corresponding to two different types of improvement, labeled  $\alpha_{\overline{\text{MS}}}(q^*)$  and  $\alpha_V(q^*)$ ], and numerical simulation values. Our results for  $N_f=2$ ,  $m_{c,\text{dressed}}^{(2)}$  and  $\kappa_{c,\text{dressed}}^{(2)}$ , are included in Tables IV and V. Comparing with the Monte Carlo estimates, we see a definite improvement over non-dressed values. At the same time, a sizable discrepancy still remains, as was expected from the start. This discrepancy sets a benchmark for lattice perturbation theory; multiplicative renormalizations, calculated to the same order and improved by cactus dressing, are expected to be much closer to their exact values. We hope to return to these calculations in a future publication.

[1] H. Panagopoulos and E. Vicari, Phys. Rev. D **58**, 114501 (1998).  
[2] H. Panagopoulos and E. Vicari, Phys. Rev. D **59**, 057503 (1999).  
[3] H. Panagopoulos and E. Vicari, Nucl. Phys. B (Proc. Suppl.) **83**, 884 (2000).  
[4] H. J. Rothe, *Lattice Gauge Theories—An Introduction* (World Scientific, Singapore, 1992).  
[5] C. Christou *et al.*, Nucl. Phys. **B525**, 387 (1998).  
[6] I. Montvay and G. Münster, *Quantum Fields on a Lattice* (Cambridge University Press, Cambridge, England, 1994).  
[7] APE Collaboration, P. Bacilieri *et al.*, Phys. Lett. B **214**, 115 (1988).

[8] JLQCD Collaboration, S. Aoki *et al.*, Phys. Rev. D **62**, 014506 (2000).  
[9] JLQCD Collaboration, S. Aoki *et al.*, Phys. Rev. D **60**, 034511 (1999).  
[10] SESAM Collaboration, N. Eicker *et al.*, Phys. Rev. D **59**, 014509 (1999).  
[11] K. M. Bitar, R. G. Edwards, U. M. Heller, and A. D. Kennedy, Nucl. Phys. B (Proc. Suppl.) **53**, 225 (1997).  
[12] G. Parisi, in *High-Energy Physics—1980*, edited by L. Durand and L. G. Pondrom, AIP Conf. Proc. No. 68 (AIP, New York, 1981).  
[13] G. P. Lepage and P. B. Mackenzie, Phys. Rev. D **48**, 2250 (1993).